Instability of Detonation Wave at Downstream of Aluminum Crimped Ribbon

Jayan Sentanuhady[1*], Willie Prasidha[1], Akmal Irfan Majid[1], Muhammad Akhsin Muflikhun[1]

[1]Departement of Mechanical and Industrial Engineering, Faculty of Engineering, Universitas Gadjah Mada, Jl. Grafika No.2, Sinduadi, Mlati, Sleman, D.I. Yogyakarta, 55281 Indonesia

Abstract. Natural gas is a very reactive fuel that easily causes a detonation wave, especially when the oxidizer is enriched with oxygen or pure oxygen. If the combustion wave is not controlled, a detonation wave can occur, which is dangerous for the safety of workers and industrial facilities. This study was conducted to develop a prototype of a detonation arrester to control detonation waves by using a detonation test tube with a total length of 3000 mm. The characteristics of the combustion wave were evaluated in the present study using a pressure sensor, an ion probe sensor, and a soot track record plate. Results showed that the propagation velocity of the combustion wave and the shock wave pressure increased, whereas the detonation cell size and the reinitiation distance decreased. The experiments performed were able to produce a shock wave pressure that was close to the Chapman–Jouguet pressure. The use of a detonation arrester model could reduce the shock wave pressure and the velocity of the combustion wave. At the initial pressure of the gas mixture of natural gas–oxygen of 10 kPa, the observed combustion phenomenon was deflagration. By contrast, when the initial pressure of the gas mixture of natural gas–oxygen was increased to 20 kPa, the observed combustion phenomenon was detonation quenching. Furthermore, increasing the initial pressure of the natural gas-oxygen mixture to 30 kPa or higher led to detonation wave propagation as the observed combustion phenomenon.

Keywords: Arrester model; Detonation quenching; Detonation reinitiation; Detonation wave

1. Introduction

Natural gas, which mainly consists of methane gas, is a fuel that is often used in industrial processes (Faramawy, Zaki, and Sakr, 2016). The use of natural gas as a fuel is also considered to fulfill energy needs in various applications, including transportation sectors, industries, and households (Supriyanto et al. 2022; Farizal, Dachyar, and Prasetya 2021; Rosyidi et al. 2020). Natural gas plays a crucial role as a transition fuel for sustainable energy systems toward a cleaner environment (Ediger and Berk, 2023; Bugaje et al., 2022; Mohammad et al., 2021; Safari et al., 2019). Meanwhile, to meet the safety standard, the design of an industrial system should consider any hazardous aspects, for example, a spontaneous fire (Thabari et al. 2023), and high propagation flame which may cause severe accidents (Hou et al., 2022; Zardasti et al., 2017; Sovacool, 2008). Interestingly, natural gas easily reacts and causes a detonation wave, particularly when the oxidizer is enriched with oxygen or pure oxygen, such as in glass-forming industries. worse conditions, the natural gas mixture may induce detonation during transport and storage (Sun and Lu, 2020b).

Detonation is a combustion wave that propagates at supersonic velocity and increases when the pressure reaches 20 to 30 times the initial pressure (Zhang *et al.*, 2020). In more detail, it is also defined as a reactive shockwave that propagates at a nearly ideal Chapman-Jouguet (CJ) velocity, trailed by chemical reactions (Lee, 2008). Consequently, the compression and ignition of the air-fuel mixture by the shockwave lead to an energy release, supports the shockwave propagation (Pan *et al.,* 2017). The detonation wave created in a combustible gas mixture can be very dangerous if it interacts with human bodies or artificial structures due to the high pressure and temperature behind the wave. The detonation behavior can be the detonation wave was quenched, and the detonation wave was initially quenched behind the block but then re-initiated again due to the focusing mechanisms of a reflected shock wave on a central axis (Obara *et al.* 2006a; 2006b). Detonation control can be applied by converting the detonation wave into the deflagration wave, which has less energy, to prevent damage caused by the detonation wave (Sun *et al.,* 2022; Ciccarelli, Johansen, and Parravani, 2011). A simple method to reduce the detonation wave is to reduce the channel diameter. The study was conducted by Gholamisheeri, Wichman, and Toulson (2017) using experiments and simulations where the detonation propagation can also be controlled in tube and obstacle geometries.

Furthermore, one of the methods that can be used to convert detonation into deflagration is to absorb the wave energy, which can be absorbed by installing the orifice or arrester in the detonation track. This method is supported by experiments using the channel geometry that can affect the flame acceleration and deflagration to detonation transition (DDT) in a detonable mixture (Azadboni *et al.*, 2017; Ettner, Vollmer, and Sattelmayer, 2014) and can be adapted without disturbing the gaseous fuel flow.

Several researchers have conducted studies of detonation propagation and control using a plate with an orifice for the hydrogen-oxygen gas mixture. Their results showed that the orifice with small holes caused the detonation quenching phenomenon. Otherwise, the presence of an obstacle in the pipeline ensured the easy and rapid development of flame acceleration from the deflagration wave to the detonation wave (Sun and Lu, 2020a; Wang *et al.*, 2018a; Rainsford, Aulakh, and Ciccarelli, 2018; Cross and Ciccarelli, 2015; Teodorczyk, Drobniak, and Dabkowski, 2009). The reinitiation of detonation is influenced by the detonation instability, which is affected by the size of the orifice or obstruction and flow velocity. Examples in this field include the reinitiation process of detonation waves behind slit-plates (Obara *et al.*, 2008), notably influenced by initial test gas pressure (Obara *et al.,* 2006b) and slit-plate configuration (Sentanuhady *et al.*, 2007). Visualization of re-initiation and quenching processes of detonation wave behind slit-plate was conducted by Obara *et al.,* (2007).

Meanwhile, metal is the best material to absorb the detonation energy since it has a high thermal conductivity. Increasing the detonation energy absorption area and thermal conductivity of the arrester can affect the effectivity of detonation quenching. These parameters can increase the heat transfer in the arrester because one of the factors that can influence detonation quenching is heat transfer (Thomas, Oakley, and Bambrey, 2020). A study using a crimped ribbon flame arrester was conducted by several scientists, and they varied the length of the arrester (see a brief review from Wang *et al.*, 2018b). Sun *et al.* (2018) numerically investigated detonation wave propagation and quenching in an in-line crimped-ribbon flame arrester, offering key insights into initiation, quenching rules, and the impact of structural parameters on propagation. Moreover, the parameters used to assess the flame arrester's effectiveness are the propagation velocity of the combustion wave, shock wave pressure, reinitiation distance, and detonation cell size.

This study aimed to observe and analyze the characteristics and combustion phenomena of natural gas–oxygen mixture with an equivalence ratio of unity through a detonation arrester model with various initial pressures (i.e., between 10 kPa and 100 kPa).

The arrester was made from an aluminum sheet with a crimped ribbon configuration. Furthermore, insights obtained from this study are expected to improve the current understanding of detonation quenching and the development of flame arrester devices.

2.   Research Methodology

This study used a detonation test tube with an inner diameter of 50 mm and a total length of 3,000 mm. The detonation test tube consisted of three parts, namely, the driver section tube, driven upstream tube, and driven downstream tube where each section has a length of 1,000 mm, respectively. The details of experimental facility can be found in our previous paper (Sentanuhady *et al.*, 2021) and only the main features are presented here. Figure 1 illustrates the schematic diagram of the detonation test equipment.

The combustion process in the driver section tube was initiated by a spark plug installed in the upstream part of the driver section. One pressure sensor (P_1; PCB Piezotronics S111A26 series) was mounted on the driven upstream tube 1,900 mm from the spark plug, and two pressure sensors (P_2 and P_3) were mounted on the driven downstream tube 2,100 and 2,200 mm from the spark plug. The pressure sensor mounted on the driven upstream tube was used to measure the amount of shock wave pressure, whereas the ion probe sensor mounted opposite the pressure sensor was used to detect the arrival time of the combustion wave.

Detonation waves can be visualized as a detonation cell structure placed along the driven downstream tube and recorded using the soot track record plate. The soot track record plate was made of 0.3 mm-thick aluminum, whose surface had a layer of film from kerosene-burning soot. Mylar film with a thickness of 0.03 mm was inserted between the driver section tube and the driven upstream tube and between the driven downstream tube and the dump tank. The arrester model was installed in a housing that was placed between the driven upstream tube and the driven downstream tube. The housing of this arrester model was 100 mm long with an inner diameter of 50 mm. In this study, a crimped ribbon flame arrester model with a length of 25.4 mm was used. The arrester model used in this study is made of aluminum with a thickness of 0.2 mm and BR = 34.6%. Here, BR (blockage ratio) is defined as the ratio of the covered metal area to the cross-sectional area of the tube used. Figure 2 shows the photograph of arrester model used in the present study.
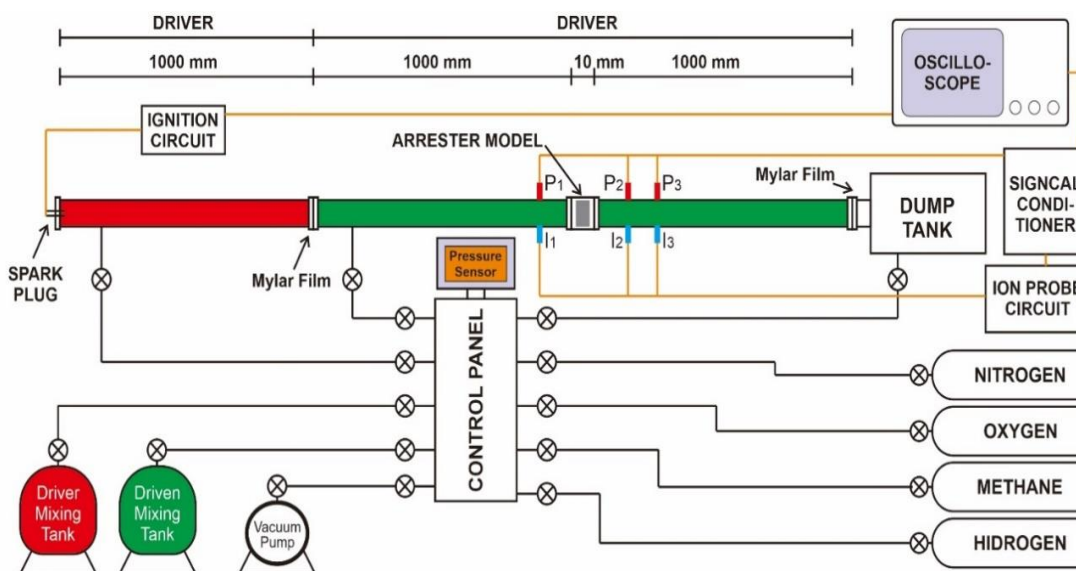

Figure 1 Schematic of the detonation test equipment
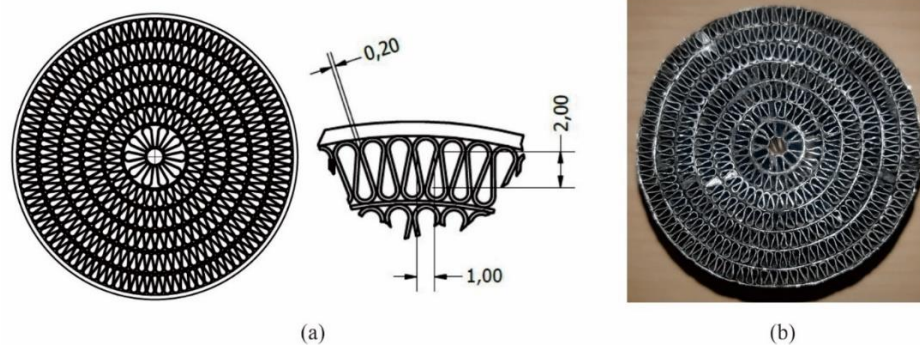
Figure 2 Arrester model (a) design and (b) postproduction

The experimental conditions applied in this study are shown in Table 1. The fuel used in the driver section tube was a stoichiometric mixture of hydrogen-oxygen at a pressure of 100 kPa, whereas the fuel used in the tube was a gas mixture of natural gas–oxygen with an equivalence ratio of unity and various initial pressures. The gas pressure used for the mixing process of both hydrogen–oxygen and natural gas–oxygen in the mixing tank, as well as the injection of the gas mixtures into the detonation test tube, is regulated and controlled using a high-precision pressure sensor. The natural gas used in this experiment is natural gas sourced from Indonesian wells that have a methane number of 96.7. In the present study, we ensure that the equipment and tools used are calibrated by the manufacturer. Thus, all the parameter testing is in the range of the equipment specification of the tools.

Table 1 Experimental conditions

Parameter	Driver section	Driven section
Fuel	Hydrogen	Natural gas
Oxidizer	Oxygen	Oxygen
Equivalence ratio	1 (stoichiometry)	1 (stoichiometry)
Initial pressure (kPa)	100	10–100, interval 10
Initial temperature (°C)	Room temperature	Room temperature
Mixing	Premixed	Premixed

3. Results and Discussion

The experimental results on the propagation of the gas mixture are presented. Without an arrester model, the natural gas-oxygen combustion wave showed two observable characteristics: deflagration waves and detonation waves. During testing with an initial pressure of 10 kPa, a deflagration wave was observed. Increasing the starting pressure to 20 kPa accelerated the combustion process, resulting in the formation of a detonation wave. Similarly, a detonation wave was formed at initial pressures above 20 kPa. The detonation waves produced within the range of 20-100 kPa can be classified into two types: unstable and stable.

An unstable detonation wave was observed at initial pressures ranging from 20 to 50 kPa, while a stable detonation wave was detected at pressures higher than 50 kPa. This is attributed to the rapid combustion reaction caused by the high initial pressure of the gas mixture (Song *et al.* 2018; Miao *et al.* 2008). Furthermore, a substantial quantity of heat energy was created, resulting in a rapid DDT formation process. The response velocity fluctuated with an unstable detonation wave, causing the detonation wave's propagation velocity to vary or be unstable. This phenomenon can be attributed to the formation of a detonation cell structure on the surface of the soot track record plate, with the instability of the detonation cell size occurring under unstable detonation wave conditions. The

combustion wave propagation mechanisms of both deflagration and detonation waves at various initial pressures are shown in Table 2.

Table 2 The propagation mechanism of combustion wave without an arrester model

Propagation mechanism	Initial pressure (kPa)
Deflagration	10
Detonation (Unstable)	20, 30, 40, 50
Detonation (Stable)	60, 70, 80, 90, 100

The installation of the detonation arrester model between the driven upstream tube and the driven downstream tube resulted in different characteristics and combustion at the downstream tube of the arrester model compared with the conditions without an arrester model. The combustion experiments using a detonation arrester model resulted in three characteristics of the combustion wave, namely, deflagration, detonation quenching, and detonation reinitiation, as listed in Table 3.

The classification of combustion wave propagation is based on the changes in the combustion wave propagation pattern that can be observed on the soot track record plate both without and with an arrester model. The detonation quenching phenomenon, which only occurred under the conditions with the arrester model, was formed because of the quenching process of the detonation waves due to heat loss through the arrester model. Thus, the combustion wave that occurred downstream of the arrester model was a deflagration wave. Along the driven downstream section of the tube, no DDT phenomenon occurred. The DDT phenomenon is the transition of the combustion wave from subsonic velocity to supersonic velocity. Furthermore, when the velocity of the detonation wave at the driven upstream tube was sufficiently high, as generally occurs at high initial pressures of the gas mixture, the combustion wave that emerges from the arrester model was a deflagration wave. This deflagration wave immediately propagated and interacted with the inner wall of the tube, converting into a detonation wave. This phenomenon is known as detonation reinitiation.

Table 2 and Table 3 indicate different propagation mechanisms because by using arrester, combustion energy will be absorbed by the arrester material. Thus, the propagation velocity of the flame is reduced. For the cases when the arrester was used, stable and non-stable detonations were not be observed. The deflagration phenomena can only be observed in the detonation quenching and detonation reinitiation in the initial pressure.

Table 3 Mechanism of the propagation of combustion wave with an arrester model

Mechanism	Initial pressure (kPa)
Deflagration	10
Detonation quenching	20
Detonation reinitiation	30, 40, 50, 60, 70, 80, 90, 100

Deflagration wave propagation without the arrester model occurred at low initial pressures. This phenomenon was observed in the experiment at a pressure of 10 kPa, as shown in Figure 3a. Notably, the combustion wave propagation occurred at all observation points (i.e., P1, P2, and P3) under the deflagration wave condition. This is characterized by the propagation of the combustion wave several microseconds after the shock wave. In experiments conducted under this condition, the shock wave pressure increased approximately 23 times from the initial pressure. Meanwhile, the velocity in positions P_2 and P_3 was 1,786 m/s, which was smaller than the Chapman–Jouguet (CJ) theoretical velocity of 2,361 m/s.

Furthermore, when the arrester model was installed in the detonation test tube, the same phenomena as that without the arrester model occurred, in which deflagration waves occurred at all observation points, as shown in Figure 3b. Moreover, the combustion wave propagated behind the shock wave at a longer distance downstream of the arrester model. The maximum pressure observed from the P_2 and P_3 sensor readings decreased when compared with the conditions without the arrester model, which was approximately 14 times the initial pressure. The propagation velocity of the combustion wave in the downstream area was also lower than that under the conditions without the arrester model, which was 1,337 m/s. This finding shows that, at an initial pressure of 10 kPa, the arrester model effectively reduces the combustion propagation velocity and pressure wave. When the initial pressure of the gas mixture of natural gas–oxygen was increased from 20 kPa to 50 kPa, under the conditions without the arrester model, the phenomenon that could be observed was the unstable propagation of the detonation wave.
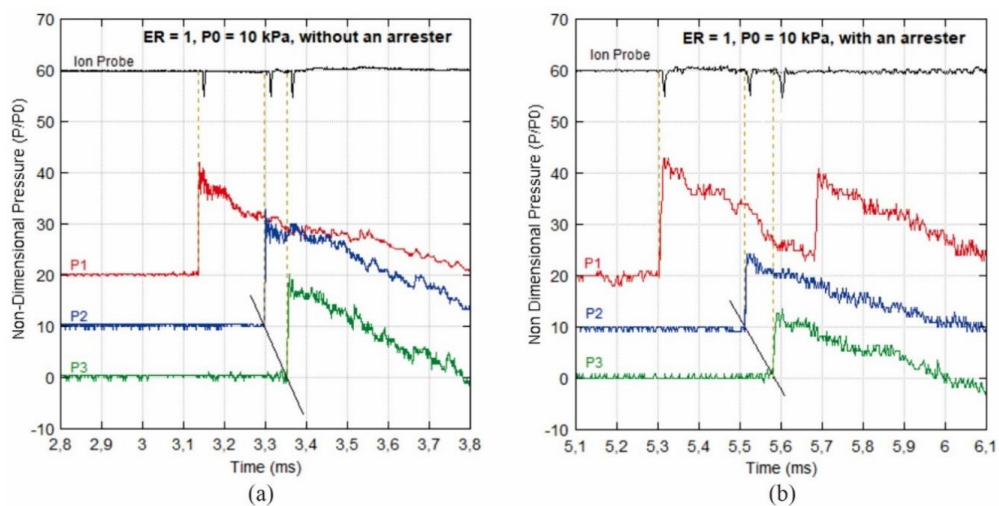

Figure 3 Pressure and ion profiles of the combustion wave with $\Phi = 1$ at an initial pressure of 10 kPa: (a) without and (b) with an arrester model

The representation of the conditions of this phenomenon is shown in Figure 4a, i.e., the pressure profile of the combustion wave along the detonation test tube without an arrester model with an initial pressure of 20 kPa. These findings show that, at position P1, which was 1,900 mm from the spark plug, the combustion wave that could be observed was the detonation wave. Furthermore, this wave would propagate downstream toward positions P2 and P3. Figure 4a shows the combustion waves at positions P2 and P3 were detonation waves.

The propagation velocity of the detonation wave between positions P2 and P3 was calculated to be 1,923 m/s, which was smaller than the CJ theoretical velocity of 2,394 m/s. However, this detonation wave was observed to propagate at an unstable velocity for the detonation cell size, which was not ideal, as shown in Figure 5a. This finding indicates that, although detonation wave propagation can be observed, the generated detonation wave was weak. The highest shock wave pressure in positions P_2 and P_3 was approximately 30 times the initial pressure. If the arrester model was attached to the detonation test tube with an initial pressure of 20 kPa, then the phenomenon that occurred was detonation quenching, as shown in Figure 5b. Notably, at the position of the P_1 sensor, the combustion wave that propagated was the detonation wave. After passing through the arrester model, the detonation wave underwent heat loss and converted into deflagration.
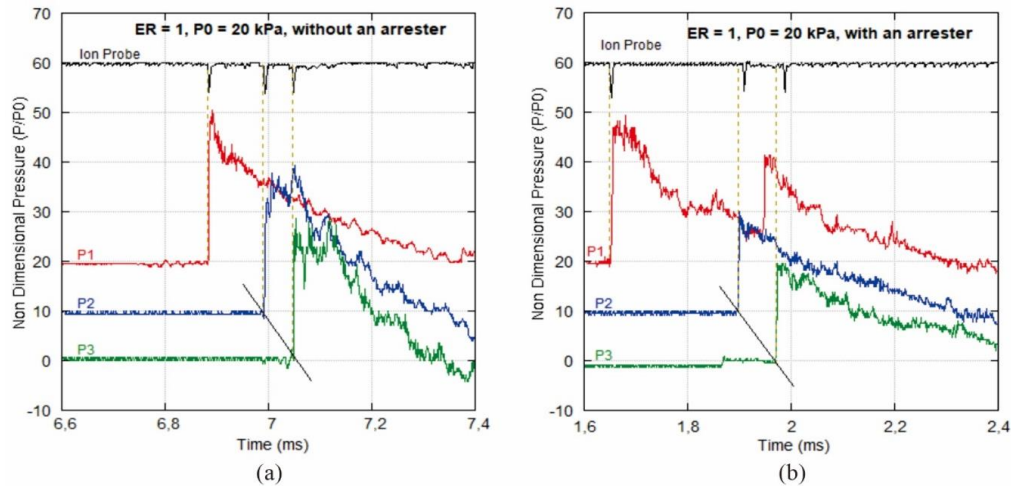
Figure 4 Pressure and ion profiles of the combustion wave with $\Phi = 1$ at an initial pressure of 20 kPa: (a) without and (b) with an arrester model
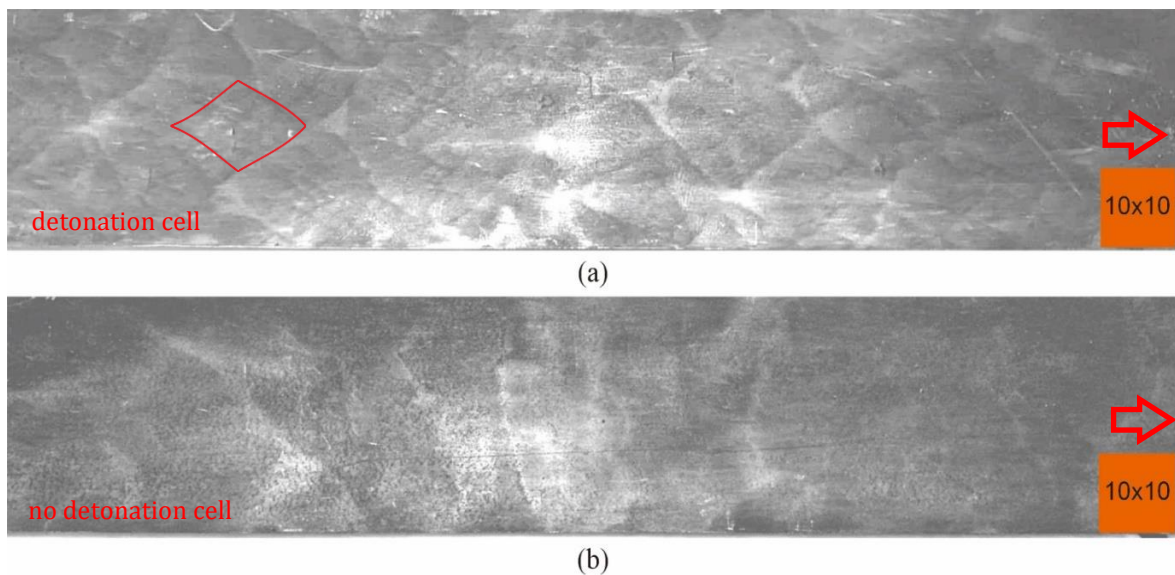

Figure 5 Visualization of the combustion wave at an initial pressure of 20 kPa: (a) without and (detonation cells appear) (b) with an arrester model (no detonation cell)

In the experiment using an arrester model, detonation reinitiation downstream of the arrester model could be observed with an initial pressure of more than 30 to 100 kPa. This phenomenon involved reinitiating the combustion wave into a detonation wave after the quenching process occurred in the downstream area of the arrester model. Figure 6a represents the detonation reinitiation phenomenon at an initial pressure of 60 kPa. Figure 6a also shows that the combustion wave at position P_1, which was upstream of the arrester model, was a detonation wave. Furthermore, after passing through the arrester model, the detonation wave was quenched and became a deflagration wave. Then, this wave propagated downstream, and at position P_3, the combustion wave was a detonation wave. This was indicated by the increasing time of the shock wave pressure and the arrival time of the combustion wave at the same time. These conditions indicate that between positions P_2 and P_3, the reinitiation process occurred, resulting in the conversion of the deflagration wave into a detonation wave that was detected at position P_3. This phenomenon was confirmed by the visualization of the soot track record on aluminum foil under the same pressure conditions in Figure 6b, where detonation reinitiation (R_1) occurred

approximately 30 mm before position P_3. The shock wave pressure downstream of the observed arrester model was the maximum pressure measured on the P_2 or P_3 sensor.

The shock wave pressure increased with the increase in the initial pressure applied. In the experiment of the gas mixture of natural gas–oxygen with an initial pressure of 20 to 100 kPa without an arrester model, the shock wave pressure was approximately close to or greater than the CJ theoretical pressure. After installing the arrester model, the shock wave pressure was smaller than the CJ theoretical pressure at all initial pressures applied, as shown in Figure 7a. Thus, using the arrester model can significantly reduce the shock wave pressure, with an average decrease of 41.5%.

Increasing the initial pressure of the gas mixture of natural gas–oxygen accelerated the molecular reactions in the gas mixture, thereby inducing a fast combustion reaction. This condition increased the momentum in the reaction process and the pressure of the shock wave, which was driven by the combustion wave. The pressure wave decreased as it passed through the arrester model, which was mostly under CJ conditions. This suggests that the arrester model effectively absorbed heat from the propagation of the detonation wave, resulting in a decrease in the combustion reaction velocity and momentum, consequently reducing the shock wave pressure far below the CJ theoretical pressure.
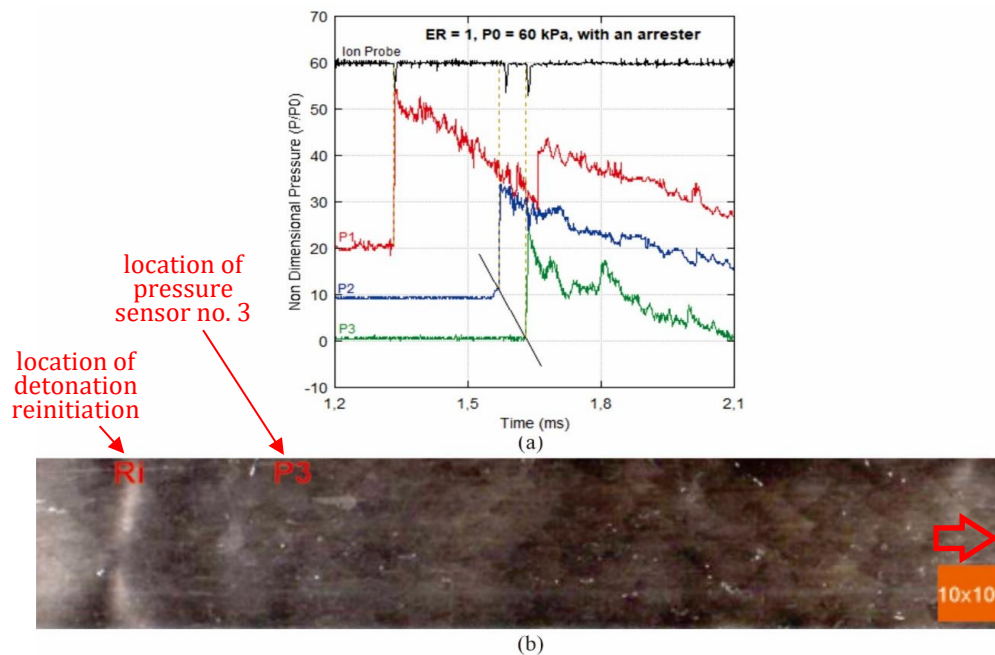

Figure 6 Characteristics of the combustion wave at an initial pressure of 60 kPa with an arrester model: (a) pressure and ion profiles of the combustion wave, (b) visualization of the combustion waves on the soot track record plate

As explained in the previous section, the reaction propagation velocity in the downstream area with an arrester model was far below the CJ theoretical velocity, as shown in Figure 7b. The graph shows the relationship between the propagation velocity of the combustion wave and the initial pressure of the gas mixture. In the experiment without the arrester model with the initial pressures of 10 and 20 kPa, the reaction velocity at the downstream area was far below the CJ theoretical velocity. However, by increasing the initial pressure from 30 kPa to 100 kPa, the reaction velocity at the downstream area was relatively nearly the same as the CJ theoretical velocity. This finding indicated that the increase in initial pressure from 30 kPa to 100 kPa produced a detonation wave where the reaction velocity was close to the CJ theoretical velocity. In terms of the stability of the detonation cells formed on the soot track record plate, the detonation wave was in an

unstable condition at an initial pressure of 30 to 50 kPa. When the initial pressure was increased to 60 to 100 kPa, the detonation wave was stable. However, at the initial pressure of 20 kPa, the reaction velocity was below the CJ theoretical velocity. Moreover, the pressure profile and soot track record indicate that the detonation wave propagation conditions were unstable.

Apart from being characterized by the propagation velocity and pressure of the shock wave, detonation wave propagation in the tube can be distinguished by analyzing the three-dimensional structure of the detonation waves formed. Each detonation wave formed an interaction with three shock waves, namely, the incident shock wave, reflected shock wave, and Mach stem. This interaction produced a hot spot that can subsequently create a detonation cell or fish scale pattern on the surface of the aluminum plate coated with soot, which is generally called a detonation cell. The detonation cell size describes the propagation velocity of the detonation waves that pass through it. The higher the detonation propagation velocity is, the smaller the detonation cell size, and vice versa. However, in this study, the propagation velocity of the detonation wave was directly proportional to the initial pressure of the gas mixture. The higher the initial pressure of the gas mixture was, the higher the propagation velocity of the detonation waves formed.
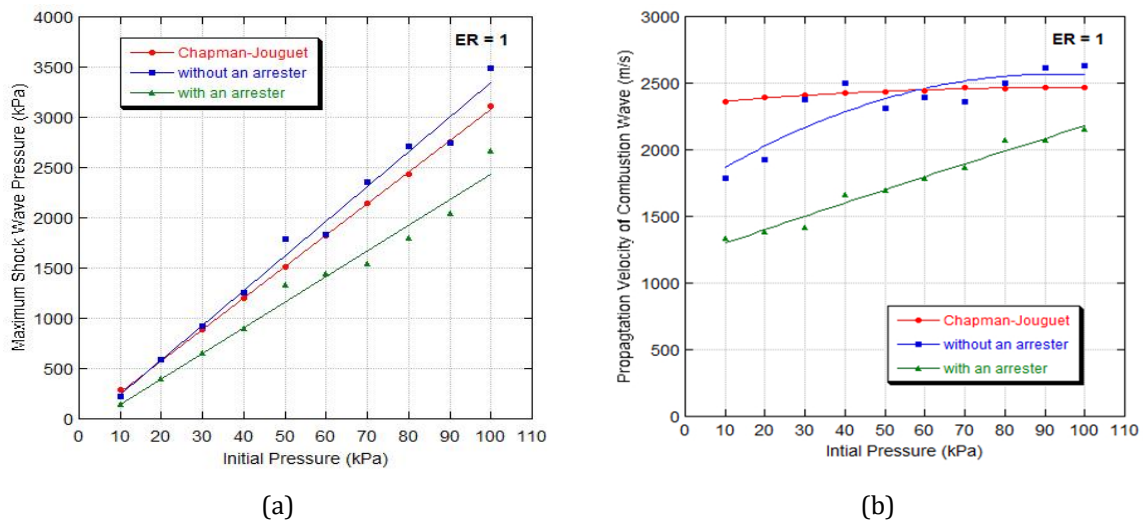

| (a) | (b) |

Figure 7 Relationship between (a) maximum shock wave pressure and initial pressure without and with an arrester model, (b) propagation velocity combustion wave and initial pressure

The horizontal and vertical axes in Figure 8a denote the initial pressure of the gas mixture in the driven section tube and the size of the detonation cells, respectively. The graph shows three curves for conditions without and with the arrester model. The condition with the arrester model tended to have a significantly larger detonation cell size than the condition without the arrester model. The average size of detonation cells with an arrester model was found to be approximately 22% larger than the average size of detonation cells without an arrester model. This finding was attributed to the fact that, at various initial pressures, the average reaction velocity with the arrester model is smaller than the average without the arrester model.
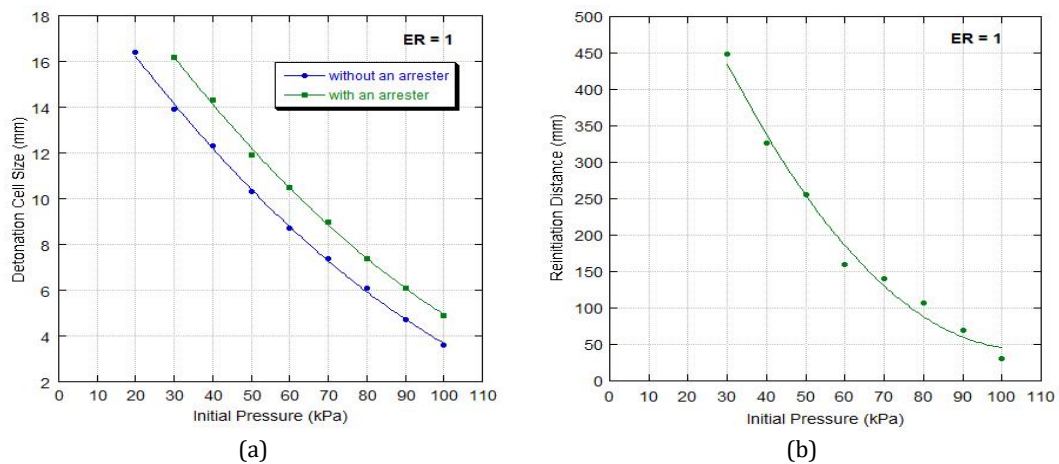
(a) (b)

Figure 8 Relationship between (a) detonation cell size and initial pressure, (b) reinitiation distance of the detonation wave and initial pressure

In the combustion experiment of the gas mixture of natural gas–oxygen with an initial pressure of 20 to 100 kPa using an arrester model, the combustion wave underwent quenching into a deflagration wave. This deflagration wave propagated downstream of the arrester model following the pressure wave. The pressure wave hit the wall of the detonation test tube and caused a hot spot on the inner surface of the wall of the detonation test tube. When the temperature was high enough, this hot spot initiated a detonation wave directly so that small detonation cells appeared around the wall. The process of forming this detonation wave is called detonation reinitiation. The distance between the location where the reinitiation occurs and the surface of the arrester model is called the detonation initiation distance. The detonation reinitiation distance is strongly influenced by the initial pressure, with the reinitiation distance decreasing with an increase in the initial pressure, as shown in Figure 8b. The increase in the initial pressure, a large amount of energy was generated from the combustion process, thereby increasing the reaction velocity and time that the pressure wave reaches the wall surface, which in turn reduced the reinitiation distance.

4. Conclusions

This study observed several characteristics and phenomena that occurred without or with an arrester model at the initial pressure of the natural gas mixture of 10 to 100 kPa, which can be utilized as design considerations for detonation arresters. The initial pressure influenced the characteristics of the combustion wave: the shock wave pressure, combustion wave propagation velocity, detonation cell size, and reinitiation distance. Increasing the initial pressure raised the shock wave pressure and combustion wave propagation velocity. Otherwise, the detonation cell size and reinitiation distance were decreased. Furthermore, the combustion process using the gas mixture of natural gas–oxygen without an arrester model with an initial pressure of 20 to 100 kPa produced a detonation wave at downstream of the arrester model. However, after installing the arrester model in the detonation test tube, the detonation wave phenomenon did not occur immediately after passing the arrester model. Instead, the detonation wave was extinguished to be a deflagration wave and reinitiated again to a detonation wave after interacting with the wall of the detonation test tube when the initial pressure was higher than 20 kPa. Otherwise, the detonation wave was quenched when the initial pressure was 20 kPa and below. The arrester also decreased the combustion wave propagation velocity by about 20%. Experiments using the arrester model have demonstrated that the arrester

model affected the combustion wave propagation process from high-risk to lower-risk propagation wave, where this method can be adapted to gas transport processes to avoid accidents.

Acknowledgments

References

Azadboni, R.K., Wen, J.X., Heidari, A., Wang, C., 2017. Numerical Modeling of Deflagration to Detonation Transition in Inhomogeneous Hydrogen/Air Mixtures. *Journal of Loss Prevention in the Process Industries*, Volume 49, pp. 722–730

Bugaje, A.B., Dioha, M.O., Abraham-Dukuma, M., Wakil, M., 2022. Rethinking The Position Of Natural Gas In A Low-Carbon Energy Transition. *Energy Research & Social Science*, Volume 90, p. 102604

Ciccarelli, G, Johansen, C.T., Parravani, M., 2011. Transition in the Propagation Mechanism During Flame Acceleration in Porous Media. *In:* Proceedings of the Combustion Institute, Volume 33, pp. 2273–2278

Cross, M., Ciccarelli, G., 2015. DDT and Detonation Propagation Limits in an Obstacle Filled Tube. *Journal of Loss Prevention in the Process Industries,* Volume 36, pp. 380–386

Ediger, V.S., Berk, I., 2023. Future Availability Of Natural Gas: Can It Support Sustainable Energy Transition? *Resources Policy*, Volume 85, Part A, p. 103824

Ettner, F., Vollmer, K.G., Sattelmayer, T., 2014. Numerical Simulation of the Deflagration-to-Detonation Transition in Inhomogeneous Mixtures. *Journal of Combustion*, Volume 2014, p. 686347

Faramawy, S., Zaki, T., Sakr, A.A.-E., 2016. Natural Gas Origin, Composition, and Processing: A Review. *Journal of Natural Gas Science and Engineering*, Volume 34, pp. 34-54

Farizal, F., Dachyar, M., Prasetya, Y., 2021. City Gas Pipeline Routing Optimization Considering Cultural Heritage and Catastrophic Risk. *International Journal of Technology*, Volume 12(5), pp. 1009–1018

Gholamisheeri, M., Wichman, I.S., Toulson, E., 2017. A Study of The Turbulent Jet Flow Field in a Methane Fueled Turbulent Jet Ignition (TJI) System. *Combustion and Flame,* Volume 183, pp. 194–206

Hou, S., Liu, Y., Wang, Z., Jing, M., Zhang, Y., Zhang., B., 2022. The Potential for Deflagration To Detonation Transition (DDT) - Lessons From LPG Tanker Transportation Accident. *Journal of Loss Prevention in the Process Industries*, Volume 80, p. 104902

Lee, J.H.S., 2008. *The Detonation Phenomenon.* England: Cambridge University Press

Miao, H., Jiao, Q., Huang, Z., Jiang, D., 2008. Effect of Initial Pressure on Laminar Combustion Characteristics of Hydrogen Enriched Natural Gas*. International Journal of Hydrogen Energy*, Volume 33(14), pp. 3876–3885

Mohammad, N., Ishak, W.W.M., Mustapa, S.I., Ayodele, B.V., 2021. Natural Gas as a Key Alternative Energy Source in Sustainable Renewable Energy Transition: A Mini Review. *Frontiers in Energy Research,* Volume 9, p. 625023

Obara, T., Sentanuhady, J., Tsukada, Y., Ohyagi, S., 2006a. A Study on Behavior of Detonation Wave Passing through Narrow Grooves. *Nippon Kikai Gakkai Ronbunshu B Hen (Transactions of the Japan Society of Mechanical Engineers Part B),* Volume 18(6), pp. 1605–1612

Obara, T., Sentanuhady, J., Tsukada, Y., Ohyagi, S., 2006b. Re-Initiation Processes of Detonation Wave behind Slit Plate (Influence of Initial Gas Pressure). *Nihon Kikai Gakkai Ronbunshu, B Hen/Transactions of the Japan Society of Mechanical Engineers*, Volume 72(12), pp. 3158–3165

Obara, T., Sentanuhady, J., Tsukada, Y., Ohyagi, S., 2008. Reinitiation Process of Detonation Wave Behind A Slit-Plate. *Shock Waves,* Volume 18, Issue 2, pp. 117–127

Obara, T., Tsukada, Y., Sentanuhady, J., Ohyagi, S., 2007. Re-Initiation Processes of Detonation Wave behind Slit Plate (Visualization of Re-Initiation and Quenching Process of Detonation Wave). *Nihon Kikai Gakkai Ronbunshu, B Hen/Transactions of the Japan Society of Mechanical Engineers*, Volume 73(11), pp. 2354–2361

Pan, Z., Chen, K., Pan, J., Zhang, P., Zhu, Y., Qi, J., 2017. An Experimental Study of The Propagation Characteristics For A Detonation Wave Of Ethylene/Oxygen In Narrow Gaps. *Experimental Thermal and Fluid Science*, Volume 88, pp. 354–360

Rainsford, G., Aulakh, D.J.S., Ciccarelli, G., 2018. Visualization of Detonation Propagation in A Round Tube Equipped with Repeating Orifice Plates. *Combustion and Flame,* Volume 198, pp. 205–221

Rosyidi, M.I., Widodo, E.M., Purnomo, T.A., Setiyo, M., Karmiadji, D.W., 2020. Converting ToD Vehicle from Gasoline to LPG in Indonesia: Cost Identification and Investment Analysis. *International Journal of Technology,* Volume 11(1), pp. 100–110

Safari, A., Das, N., Langhelle, O., Roy, J., Assadi, M., 2019. Natural Gas: A Transition Fuel for Sustainable Energy System Transformation? *Energy Science & Engineering*, Volume 7 (4), pp. 1075–1094

Sentanuhady, J., Obara, T., Tsukada, Y., Ohyagi, S., 2007. Re-Inititaion Processes of Detonation Wave behind Slit Plate (Influence of Slit-Plate Configuration). *Nihon Kikai Gakkai Ronbunshu, B Hen/Transactions of the Japan Society of Mechanical Engineers*, Volume 73, Issue 8, pp. 1737–1744

Sentanuhady, J., Tuasikal, J.A., Prasidha, W.,, Majid, A.I., 2021. The Characteristics of LPG Detonation Wave Propagation Behind Porous Media Model. *IOP Conf. Ser: Mater. Sci. Eng.*, Volume 1096, p. 012040

Song, Z., Zhang, X., Hou, X., Li, M., 2018. Effect of Initial Pressure, Temperature and Equivalence Ratios on Laminar Combustion Characteristics of Hydrogen Enriched Natural Gas. *Journal of the Energy Institute*, Volume 91(6), pp. 887–893

Sovacool, B.K., 2008. The Costs of Failure: A Preliminary Assessment of Major Energy Accidents, 1907–2007. *Energy Policy*, Volume 36, pp. 1802–1820

Sun, S., Liu, G., Shu, Y., Ye, C., Deng, J., 2022. Effect Of Flame Speed And Explosion Pressure On Flame Quenching Performance For In-Line Crimped-Ribbon Flame Arresters. *Cogent Engineering*, Volume 9 (1), p. 2118651

Sun, S.C., Shu, Y., Feng, Y., Sun, D.C., Long, H.T., Bi, M.S., 2018, Numerical Simulation Of Detonation Wave Propagation And Quenching Process In In-Line Crimped-Ribbon Flame Arrester. *Cogent Engineering*, Volume 5(1), p. 1469377

Sun, X., Lu, S., 2020a. Effect of Obstacle Thickness on the Propagation Mechanisms of a Detonation Wave. *Energy,* Volume 198, p. 117186

Sun, X., Lu, S., 2020b. Experimental Study of Detonation Limits in CH_4-$2H_2$-$3O_2$ Mixtures: Effect of Different Geometric Constrictions. *Process Safety and Environmental Protection,* Volume 142, pp. 56–62

Supriyanto, E., Sentanuhady, J., Hasan, W.H., Nugraha, A.D., Muflikhun, M.A., 2022. Policy and Strategies of Tariff Incentives Related to Renewable Energy: Comparison between Indonesia and Other Developing and Developed Countries. *Sustainability*, Volume 14(20), p. 13442

Teodorczyk, A., Drobniak, P., Dabkowski, A., 2009. Fast Turbulent Deflagration and DDT of Hydrogen-Air Mixtures in Small Obstructed Channel. *International Journal of Hydrogen Energy*, Volume 34(14), pp. 5887–5893

Thabari, J.A., Auzani, A.S., Nirbito, W., Muharam, Y., Nugroho, Y.S., 2023. Modeling of Coal Spontaneous Fire in A Large-Scale Stockpile. *International Journal of Technology,* Volume 14(2), pp. 257–266

Thomas, G., Oakley, G., Bambrey, R., 2020. Fundamental Studies of Explosion Arrester Mitigation Mechanisms. *Process Safety and Environmental Protection*, Volume 137, pp. 15–33

Wang, L.Q., Ma, H.H., Shen, Z.W., Chen, D.G. 2018b. Flame Quenching By Crimped Ribbon Flame Arrestor: A Brief Review. *Process Safety Progress,* Volume 38(1), pp. 27–41

Wang, L.Q., Ma, H.H., Shen, Z.W., Lin, M.J., Li, X.J., 2018a. Experimental Study of Detonation Propagation in A Square Tube Filled with Orifice Plates. *International Journal of Hydrogen Energy,* Volume 43(9), pp. 4645–4656

Zardasti, L., Yahaya, N., Valipour, A., Rashid, A.S.A., Noor, N.Md., 2017. Review On The Identification Of Reputation Loss Indicators In An Onshore Pipeline Explosion Event, *Journal of Loss Prevention in the Process Industries,* Volume 48, pp. 71–86

Zhang, B., Liu, H., Yan, B., Ng, H.D., 2020. Experimental Study of Detonation Limits in Methane-Oxygen Mixtures: Determining Tube Scale and Initial Pressure Effects. *Fuel,* Volume 259, p. 116220